

See discussions, stats, and author profiles for this publication at: <https://www.researchgate.net/publication/6931645>

Pressure-Induced Polymerization in Solid Ethylene

ARTICLE *in* THE JOURNAL OF PHYSICAL CHEMISTRY B · DECEMBER 2005

Impact Factor: 3.3 · DOI: 10.1021/jp0536495 · Source: PubMed

CITATIONS

40

READS

47

5 AUTHORS, INCLUDING:



David Chelazzi

University of Florence

29 PUBLICATIONS 269 CITATIONS

SEE PROFILE



Mario Santoro

Italian National Research Council

59 PUBLICATIONS 1,398 CITATIONS

SEE PROFILE



Vincenzo Schettino

University of Florence

195 PUBLICATIONS 3,496 CITATIONS

SEE PROFILE

Pressure-Induced Polymerization in Solid Ethylene

David Chelazzi,[†] Matteo Ceppatelli,^{†,‡} Mario Santoro,[‡] Roberto Bini,^{*,†,‡} and Vincenzo Schettino^{†,‡}

LENS, European Laboratory for Non-Linear Spectroscopy and INFM, Via N. Carrara 1, I-50019, Sesto Fiorentino (FI), Italy, and Dipartimento di Chimica, Università degli Studi di Firenze, Via della Lastruccia 3, I-50019, Sesto Fiorentino (FI), Italy

Received: July 4, 2005; In Final Form: September 9, 2005

Ethylene is the simplest organic molecule containing a double bond and is the starting monomeric unit in the synthesis of polyethylene, one of the most largely produced polymers. Here we report a high pressure infrared study of ethylene at room temperature. A polymerization reaction is observed when the crystalline phase I is compressed above 3.0 GPa. The reaction kinetics was investigated at two different pressures, 3.6 and 5.4 GPa. The recovered product was identified in both cases as polyethylene, but while a conformationally disordered and branched low-density polymer is obtained at the highest pressure, a high-density crystalline polymer is obtained at 3.6 GPa. A reaction mechanism was proposed on the basis of the kinetic data and the structural information.

1. Introduction

The high pressure behavior of simple molecules is of paramount importance in many research fields dealing with condensed matter like material science, planetary science, chemistry and geophysics. The physical and chemical properties of these systems can be substantially modified depending on the thermodynamic conditions. As the pressure is concerned, different changes can be induced depending on the molecular complexity and on the range where the pressure is tuned. Solid–solid phase transitions generally precede more dramatic electronic changes such as reversible insulator-to-metal transitions and molecular–nonmolecular transformations or irreversible chemical reactions. The occurrence of these processes is due to the high compressibility of these systems and to the consequent large effect of pressure that effectively tunes the intermolecular interactions making them comparable to the intramolecular ones. Up to now, several examples of such pressure-induced reactions have been reported for unsaturated molecular systems,^{1,2} and hydrocarbons in particular, all of them concerning condensation processes: addition, polymerization, and amorphization. In some cases, very selective and quantitative processes have been observed at high pressure depending on the specific molecular geometry, such as the deformation following an electronic excitation, or on the constraints imposed by the steric hindrance in the crystal arrangement.^{3,4} The interest in these high-pressure syntheses is 2-fold. First, new materials of technological interest recoverable at ambient conditions can be obtained; second, the employment of any solvent, catalyst, or initiator can be avoided without affecting the efficiency and the selectivity of the process. Therefore, the study of these processes represents an important tool for extending our knowledge beyond ambient and low-pressure chemistry, understanding condensed phase reactivity, testing theoretical models, and also establishing new synthetic routes with a reduced environmental impact.

Ethylene is the simplest organic molecule containing a double bond, and it is the starting monomeric unit in the synthesis of polyethylene, one of the most largely produced polymer. The parameter affecting the mechanical properties of polyethylene, and hence its applications, is the degree of crystallinity that is correlated to the density. The higher the crystallinity, the higher the mechanical and thermal resistance of the material. The pressure-induced reaction of ethylene was reported by Wield-raijer et al. at 2.5 GPa and 330 K as they observed the polymerization of ethylene by means of calorimetric measurements.⁵ Nevertheless, neither the reaction mechanism was investigated nor the reaction product was characterized. We have recently shown that crystalline polyethylene of outstanding quality can be produced from liquid ethylene between 0.2 and 0.7 GPa at ambient temperature with an optical catalysis, therefore, by using only physical methods like pressure and light.⁶

In the present work, we focused our attention on the reactivity of ethylene in the solid phase. The fixed positions and relative orientation of molecules in the crystal pose additional constraints to the molecular interaction and can possibly open preferential reaction paths. It will be shown that at lower pressure (3.6 GPa) a linear growth process is induced with the production of a high-density crystalline polymer, while a more complex evolution of the growth process, leading to a low-density polyethylene, is revealed at higher pressure (5.4 GPa). This change of the mechanism is interpreted in terms of the anisotropic compressibility of crystalline ethylene. The polymerization in the crystal is compared with the light-catalyzed reaction in the liquid.

2. Experimental Setup

Ethylene was compressed by means of a membrane diamond anvil cell (MDAC) equipped with Ila type diamonds. The sample was laterally retained by a stainless steel gasket. The initial sample dimensions were about 150 μm in diameter and 50 μm in thickness. The cell was loaded in a nitrogen inert atmosphere by condensing ethylene (purity 99% from Rivoira) directly on the diamonds, below the melting temperature (104 K). The deposition line was pumped and purged in order to

* Corresponding author. Università degli Studi di Firenze.

[†] Università degli Studi di Firenze.

[‡] LENS and INFM.

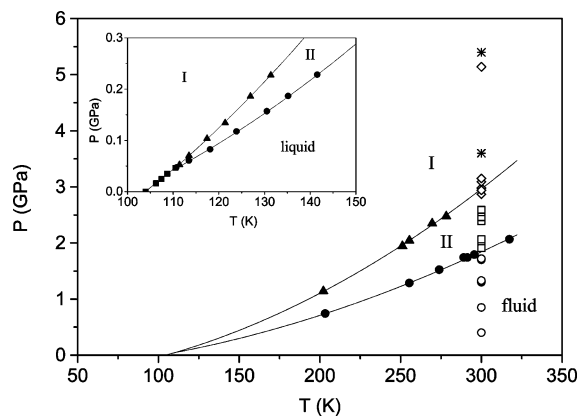


Figure 1. Phase diagram of ethylene. Full symbols indicate the phase boundaries and are from refs. 5, 10, 11. Empty symbols indicate the P–T conditions where the characteristic spectra of the fluid (circles), of the phase II (squares) and of the phase I (diamonds) have been measured in this work during compression experiments. Stars identify the P–T conditions where the reaction was studied.

avoid water contamination and for this purpose a P_2O_5 filter was also placed just before the outlet of the line. A ruby chip was inserted in the sample to perform in situ pressure measurements by the R_1 ruby fluorescence band shift.⁷ As excitation source, a few milliwatts of the duplicated 532 nm line of a Nd:YAG laser were used. The possibility of an active role of the 532 nm laser radiation in the catalysis of the reaction at the powers employed for the ruby calibration has been checked and excluded. Infrared absorption spectroscopy was employed to monitor the reaction and to characterize the product. A FTIR spectrometer (Bruker IFS-120 HR) specifically modified to host a DAC and a dedicated beam condenser, was employed.^{8,9} The instrumental resolution chosen for the experiments was better than 1 cm^{-1} . During all the experiments the pressure was increased in steps of 0.2–0.3 GPa, waiting at least 15 h in order to monitor any change in the IR spectrum of ethylene. The reaction product was also investigated by means of Raman spectroscopy, using the 514.5 nm line of an Ar ion laser. The Raman signal was collected in a backscattering configuration, filtered by a triple monochromator (Acton TR555) and measured by a liquid nitrogen cooled CCD detector. The IR and Raman spectra of the samples recovered from the high-pressure experiments have been compared with commercial polyethylene from Sigma-Aldrich.

3. Phase Transitions

The phase diagram of ethylene (see Figure 1) has been characterized at high pressure by NMR (0–2.5 kbar, 100–140 K),¹⁰ isochoric (up to 2.3 GPa and 322 K),⁵ and differential scanning calorimetry (up to 2.3 GPa and 300 K)¹¹ measurements; while X-ray,¹² neutron scattering,¹³ IR spectra,¹⁴ and calculations¹⁵ were employed at ambient pressure. Two solid phases have been identified. For pressures and temperatures lower than 468 bar and 110.36 K, respectively, liquid ethylene solidifies into an ordered crystal phase, indicated as phase I and having monoclinic crystal structure with space group $P2_1/n$ and two molecules per unit cell.^{12,13} With increasing pressure above 110.36 K, ethylene crystallizes in another solid phase, indicated as phase II,^{5,10,11} which was identified as plastic, i.e., characterized by orientational disorder, and whose structure was assigned to space group $Im3m$.¹³ The ordered phase I is obtained once phase II is further compressed.

The room-temperature evolution of the IR spectrum along increasing pressure is reported in Figure 2. The first trace,

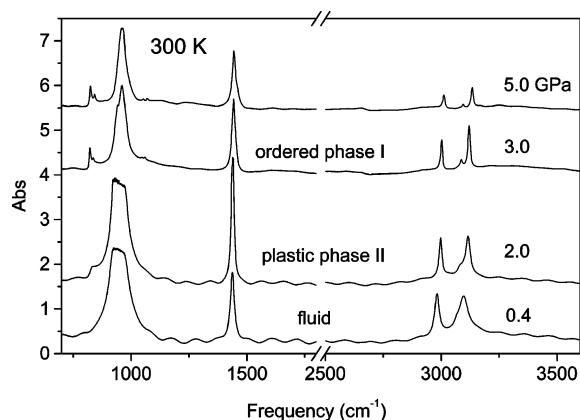


Figure 2. Pressure evolution of the IR spectrum of ethylene along a room-temperature isotherm.

measured at 0.4 GPa in the fluid phase, consists of an out of scale absorption at about 950 cm^{-1} , assigned to the ν_7 (b_{1u} , CH_2 wagging), and other three strong absorptions at 1437, 2982, and 3097 cm^{-1} , assigned to the ν_{12} (b_{3u} , CH_2 bending), ν_{11} (b_{3u} , CH stretching) and ν_9 (b_{2u} , CH stretching) modes, respectively. Finally, the ν_{10} (b_{2u} , CH_2 rocking) mode, which has very low intensity in the gas phase,¹⁶ is observed in the spectrum of fluid ethylene only above 0.9 GPa as a weak absorption at 833 cm^{-1} . Around 1.8–1.9 GPa, the broad asymmetric band between 3070 and 3100 cm^{-1} , assigned to the ν_9 and to the $\nu_{12} + \nu_2$ combination modes, starts to separate into a doublet. Above 2.6 GPa, a sudden drop of the sample pressure from 2.7 to 2.4 GPa is measured while the weak band at 833 cm^{-1} splits in two components, 822 and 836 cm^{-1} , and a weak doublet appears at 1048 and 1062 cm^{-1} in the region of the $\nu_4(a_u)$ mode that is IR inactive in the isolated molecule. Also the ν_{12} band at 1437 cm^{-1} is not symmetric anymore and reveals the presence of two unresolved components at 1443 and 1453 cm^{-1} . Finally in the CH stretching region the ν_9 and $\nu_{12} + \nu_2$ unresolved absorption bands separate into two distinct components.

According to these observations the transition between phase II and the ordered crystal phase I is easily detected from the spectra, due to the appearance of Davydov splittings for most of the modes, and from the frequency discontinuities measured at the transition for the modes reported in Figure 3. Also the transition from the fluid to the disordered solid-phase II was detected by the frequency discontinuity (about 0.8 cm^{-1}) and the slope change observed at 1.8 GPa in the pressure shift of the ν_{12} mode (see Figure 3). The literature data report the ambient pressure crystal structure of phase I to be $P2_1/n$ with 2 molecules per unit cell sitting on a C_i site and with a C_{2h} factor group. According to this structure no activity of the g modes of the isolated molecule should be observed in the IR spectrum and every u mode is expected to split in two components, and that is indeed what we observed.

4. The Chemical Reaction

The occurrence of a reaction induced by pressure was first reported at 322 K and 2.3 GPa by Wieldraijer et al. by means of isochoric measurements.⁵ The reaction was identified as a polymerization by the observation in the IR spectrum of characteristic bands due to the polymer and of the simultaneous weakening of those assigned to the monomer. At room-temperature, ethylene reacts for pressures higher than 3.0 GPa. We have studied the evolution with time of the IR spectrum at room temperature and two different pressures, 3.6 and 5.4 GPa. Fresh liquid samples were rapidly compressed up to the desired

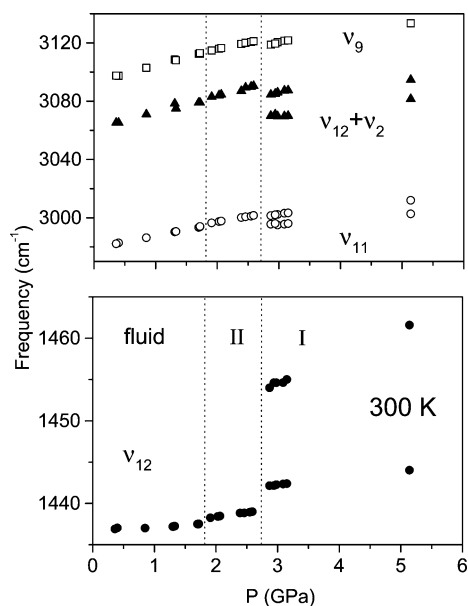


Figure 3. Pressure shift of the ν_{12} CH₂ bending mode (lower panel), of the fundamentals ν_9 (empty squares) and ν_{11} (empty circles), and of the combination ($\nu_2 + \nu_{12}$) in the CH stretching region (upper panel). All the data have been collected in compression experiments.

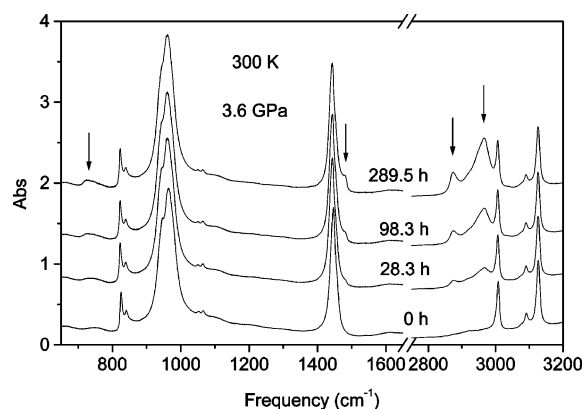


Figure 4. Time evolution of the IR spectra during the reaction at 300 K and 3.6 GPa. Arrows indicate the polymer peaks forming during the reaction.

pressure. The first changes in the IR spectra, indicating the occurrence of the reaction, were observed after ~ 30 h at 3.6 GPa, while this induction time is reduced to ~ 10 h at 5.4 GPa. The pressure was kept constant during the entire experiment and the spectra were acquired for 289 h at 3.6 GPa and 719 h at 5.4 GPa. In both cases part of the monomer was still present in the cell when the experiment was stopped, indicating that the reaction was not complete. Nevertheless, a considerable amount of a white/transparent plastic solid was recovered at ambient condition, thus confirming the previous observation concerning the polymer formation. The new IR bands growing during the reaction are observed in the region between 2850 and 3000 cm^{-1} , assigned to CH stretching modes involving saturated C atoms, at 1482 cm^{-1} on the high-frequency side of the ν_{12} band, and in the C–H bending region at 720 cm^{-1} (see Figure 4). These bands are the most intense in the IR spectrum of polyethylene whose complete assignment is reported in Table 1. The obtainment of the polymer is also confirmed by the comparison of the IR and Raman spectra of the recovered product with the spectra of commercial polyethylenes having different degree of crystallinity and densities.

Polyethylene is always obtained as a mixture of amorphous and crystalline fractions, with their relative amounts being the

TABLE 1: IR (u) and Raman (g) Active Vibrational Modes of Crystalline Polyethylene

mode	frequency (cm^{-1})	description
b_{1u}	80 ^a	trasl. a axis
b_{3g}	105 ^a	libr.
b_{2u}	109 ^a	trasl. b axis
a_g	136 ^a	libr.
b_{2u}	720 A	$\gamma_r(\text{CH}_2)$
b_{1u}	731	
a_g	1168	
b_{3u}	1050	$\gamma_t(\text{CH}_2)$
b_{2g}	1295 (1303 A)	
b_{2g}	1061 (1078 A)	$\nu_+(0)$
a_g	1131 (1303 A)	$\nu_+(\pi)$
b_{3u}	1176	$\gamma_w(\text{CH}_2)$
b_{2g}	1415	
a_g	1442 (1440 A)	$\delta(\text{CH}_2)$
b_{2u}	1463 A	
b_{3g}	1468	
b_{1u}	1473	
a_g	2848	$\nu_{ss}(\text{CH}_2)$
b_{1u}	2850 A	
b_{2u}	2857 A	
a_g	2883 A	$\nu_{aa}(\text{CH}_2)$
b_{2u}	2899 A	
b_{1u}	2924 A	

^a Data from lattice phonon spectra measured at 5 K;¹⁷ all the other frequencies are obtained at room temperature.¹⁸ A indicates the frequencies where also the bands of amorphous polyethylene are found.

key parameter to classify the synthetic method. The quality of the polymer is generally determined according to the density, which increases with the crystalline fraction. The higher the density, the higher is the polymer quality, and hence the thermal and mechanical resistance properties of the material. The crystal structure of polyethylene is orthorhombic, P_{nam} , with two units per cell. A perfect molecular packing is ensured in the ordered crystal by the linearity of the polymeric units through configurational periodicity and conformational regularity. On the other side, in the amorphous domains the conformational irregularities prevent an ordered molecular packing and decrease the density.¹⁹ Vibrational spectroscopy is a powerful tool in revealing the degree of crystallinity of polyethylene. Characteristic bands have been identified and assigned to crystalline and amorphous polyethylene both in IR^{20,21} and Raman spectra.^{18,22}

The IR spectra of the two recovered products have been compared to a high-density (0.966 g cm^{-3}) and a low-density (0.922 g cm^{-3}) commercial polyethylene from Aldrich. Three spectral regions are significant in revealing the crystallinity of polyethylene (see Figure 5). The first region extends from 680 to 760 cm^{-1} and involves a doublet due to the Davydov splitting of the CH₂ rocking mode of polyethylene. This doublet is more resolved in high density polymers than in the low density ones according to the higher degree of crystallinity. The sample recovered from the reaction at 3.6 GPa presents a nicely resolved doublet while the two peaks are only scarcely resolved in the product recovered from the 5.4 GPa reaction. The information gained by the comparison of the IR spectra is more straightforward in the region extending between 1250 and 1400 cm^{-1} where the absorption is essentially due to the amorphous domains. The three broad bands observed in all the spectra are due to the amorphous fraction and are assigned to twisting (1303 cm^{-1}) and wagging (1353 and 1369 cm^{-1}) modes of CH₂–CH₂ units having gauche configuration.¹⁸ The sharper peak, observed at 1378 cm^{-1} in the low density commercial polymer and in the recovered material from the high pressure reaction, is hardly detectable in the high-density polymer and in the low-pressure product. This peak is characteristic of the symmetric

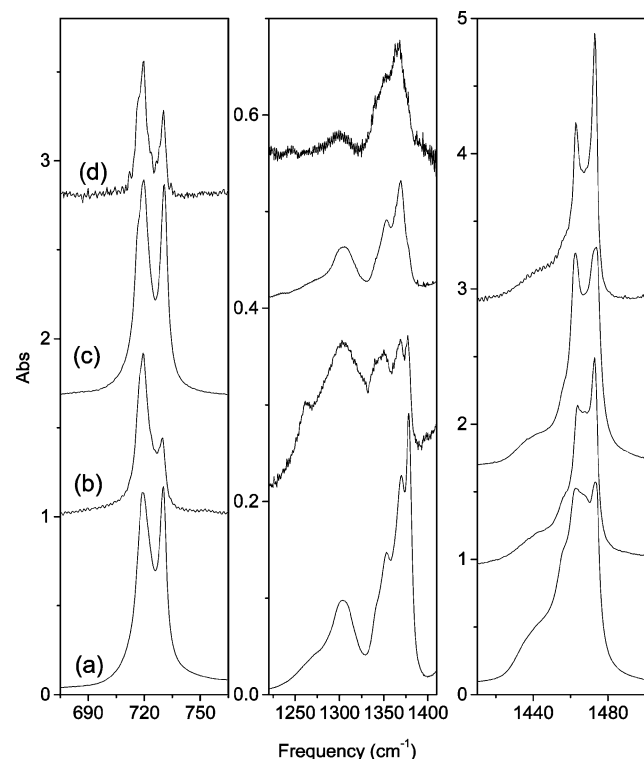


Figure 5. Comparison of selected regions of the IR spectra measured in the polymers recovered from the reaction in the solid phase at 3.6 (d) and 5.4 (b) GPa with those of commercial (c) high (0.966 g/cm³) and (a) low density (0.922 g/cm³) polyethylenes from Aldrich.

bending of CH₃ groups thus indicating in these polyethylenes the presence of a considerable amount of chain terminations which implies, according to the stoichiometry of the system, a chain branching and consequently a reduced length of the chains. The third region, between 1420 and 1500 cm⁻¹, is characterized by the doublet at 1473 and 1463 cm⁻¹ assigned to the crystal field splitting of the CH₂ bending mode. In the low density polyethylene, and in the polyethylene recovered from the reaction in the crystal at 5.4 GPa, these two components are poorly resolved and show comparable intensities. A better resolution of these peaks is achieved in the commercial high density polymer and, particularly, in the low pressure product. In the latter material, the bandwidths appear definitely sharper than in the other polymers. The broad band underlying the crystal doublet and peaked at about 1440 cm⁻¹ is weaker in the high density polymer and in the sample recovered from the low pressure reaction while becomes more evident in the other two polymers. This peak is due to gauche defects, and its broadness is attributed to the presence of different gauche structures constrained by the polymer lattice. From the comparison of the IR spectra, it is therefore possible to conclude that the polymers produced by compressing solid ethylene are rather different. The polymer produced at 3.6 GPa is very similar to the high density polyethylene with a negligible amount of chain terminations and nicely resolved crystal components thus suggesting a high degree of crystallinity. On the contrary, the spectrum of the material recovered from the reaction at 5.4 GPa is comparable to that of low-density polyethylene from Aldrich.

The Raman spectra recorded on the same samples (see Figure 6) confirm the information gained by the IR data. The two broad bands at 1078 and 1310 cm⁻¹ observed in the low-density polyethylene and in the sample recovered from the 5.4 GPa reaction indicate the presence of amorphous domains being assigned to the skeletal C–C stretching and to the gauche CH₂–

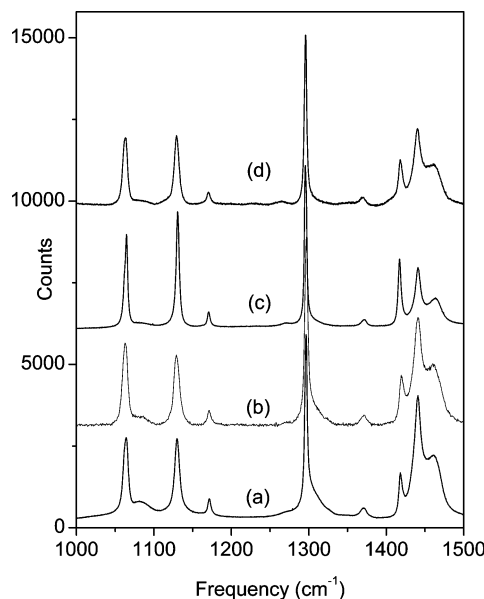


Figure 6. Comparison of the Raman spectra measured in the polymers recovered from the reaction in the solid phase at 3.6 (d) and 5.4 (b) GPa with those of commercial (c) high (0.966 g/cm³) and (a) low density (0.922 g/cm³) polyethylenes from Aldrich.

CH₂ unit bending, respectively.^{18,22} The low-frequency component, around 1415 cm⁻¹, of the triplet lying between 1400 and 1500 cm⁻¹ is indicated as a marker of the sample crystallinity. The intensity of this band and its resolution from the higher frequency doublet are reported to increase with the degree of crystallinity.²²

With regard to the mechanism of the chemical reaction, we gained information about the kinetics of the process by the analysis of the time evolution of the IR absorption bands forming during the reaction and due to C–H stretching involving sp³ C atoms. This spectral region was selected because the bands of the reaction product are very strong and can be detected since the early stages of the reaction. Four polyethylene bands grow in this region (see Figure 4) and are assigned to two fundamentals (CH₂ symmetric stretching at 2878 cm⁻¹ and CH₂ antisymmetric stretching at 2968 cm⁻¹) and to two combination modes (2916 and 2944 cm⁻¹). The absorbance of these bands was the parameter used to extract the kinetic information on the process. The four peaks are quite broad and overlapped so that some arbitrariness can be introduced in the fit procedure. For this reason, we used the total integrated absorption of the four bands. The model adopted to reproduce the kinetic data, first developed by Avrami, concerns diffusion-controlled solid-state reactions,²³ and its general formulation is expressed by the following equation:

$$\frac{A_t}{A_\infty} = 1 - e^{-[k(t-t_0)]^n} \quad (1)$$

Here A_t and A_∞ are the band intensities at the time t and at the end of the reaction, respectively; t_0 is the initial time related to the nucleation step, k is the rate constant, and n is a parameter according to which the dimensionality of the growth process can be extracted. Pseudo Voigt band shapes were employed to reproduce the absorption profile and the time evolution of the integrated absorption was fitted according to eq 1. The results are reported in Figure 7 for the experiments at 3.6 and 5.4 GPa. At 3.6 GPa, the experimental data have been fitted by using a value of the n parameter of 0.4, indicating a diffusion-controlled linear growth of the chain.²³ It should be recalled that, as already

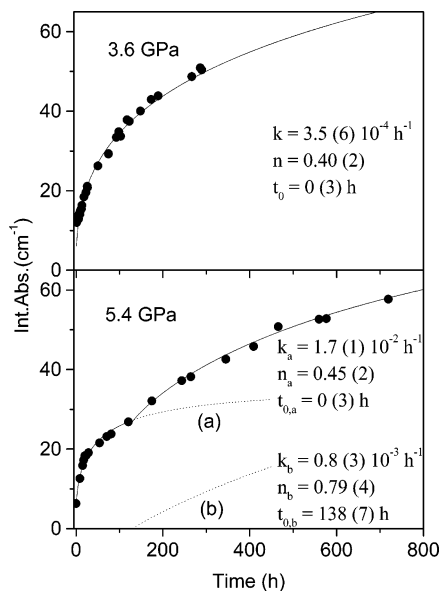


Figure 7. Room-temperature time evolution of the integrated absorption of CH stretching IR bands of the reaction product measured at 3.6 GPa (upper panel) and 5.4 GPa (lower panel). The evolution at 3.6 GPa has been reproduced according to eq 1, while the fitting curve employed at 5.4 GPa is the sum of two distinct growth processes (a, b) of the type reported in eq 1.

demonstrated in the case of acetylene,²⁴ butadiene,⁴ and CO₂,²⁵ the diffusion step should be interpreted as due to the lattice motions that continuously modulate the relative orientations and distances of the molecules in the crystal leading to instantaneous configurations that allow the chemical reaction to occur. At 5.4 GPa the kinetic curve is remarkably different from that at 3.6 GPa. The absorbance values steeply increase at short reaction times and a discontinuity is observed around 125 h. The overall behavior can be reproduced only by taking into account two distinct growth processes. In the first, used to reproduce the experimental data at short times, the fit parameters indicate a linear growth ($n = 0.45$) with a rate constant 2 orders of magnitude larger than the one measured at 3.6 GPa. The second process is slower and starts to contribute at 138 h. The larger n value (0.79) obtained for this process suggests an increased dimensionality of the polymer growth²³ possibly related to the branching of the chains or to the formation of conformational defects in the polymer propagation.

According to the crystal structure of phase I (C_{2h} , $Z = 2$)¹² (Figure 8) the polymer growth should likely involve the ethylene molecules located along the a axis because of the shortest C—C distance (3.646 Å at room pressure) between nearest neighbor molecules and the reduced angular rearrangement (CCC angle of 131°) required to give the tetrahedral hybridization of the C atoms in the polymer. However, neutron experiments at 99 K have shown a huge reduction of the cell along the b axis (16.7%) in comparison to those along the a and c axis (~2%) when the sample is compressed at 0.2 GPa.¹³ This anisotropic compressibility makes the distances between C atoms of the nearest neighbor molecules located along the a axis (3.527 Å) comparable to those between the molecules sitting on the vertex and at the center of the cell (3.635 Å). This effect, joined to the similar relative orientation in the two cases with respect to the tetrahedral arrangement required for the polymer formation, being the CCC angles 131 and 83°, respectively, suggests a progressive decrease in the selectivity of the reaction process with rising pressure. This observation is also consistent with the results of the kinetic analysis and of the IR and Raman results. In the higher pressure experiment, the kinetic data

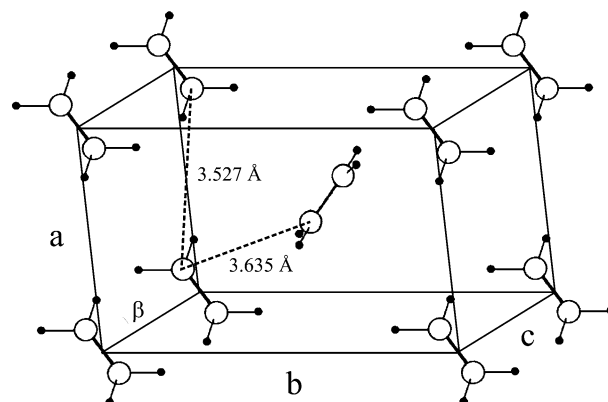


Figure 8. Unit cell of crystalline ethylene in phase I ($P2_1/n$, C_{2h}^5 , $Z = 2$). The lattice constants at 0.2 GPa and 99 K¹³ are $a = 4.506$ Å, $b = 5.558$ Å, and $c = 3.977$ Å. The monoclinic angle, $\beta = 94.4^\circ$, and the molecular orientation are available only at room pressure and 85 K,¹² being the angle formed by the C=C bond with the a axis and the ab plane at 36 and 14.6°, respectively. In the figure, the C—C distances between nearest neighbor molecules are also reported.

indicate an increase in the dimensionality of the growth process, while the IR spectra of the recovered polymer show a clear intensification of the bands due to gauche conformational defects and methylic chain terminations. These experimental results can be explained with a greater abundance of defects due to the bending and the branching of the polymeric chains in the sample recovered from the higher pressure experiment. The two different kinetic regimes observed in the 5.4 GPa experiment could be therefore interpreted according to two competitive effects. With rising pressure the formation of many nuclei is favored, speeding up the transformation in the first stages of the kinetics. In addition, the growth process is less selective with respect to lower pressure conditions because it can occur along both directions, namely the a axis and the diagonal of the unit cell, so that ramification and formation of conformational defects will occur, establishing an intrinsic limit to the chain lengthening. Furthermore, the higher density, corresponding to a greater steric hindrance, makes more difficult the rearrangement required by the hybridization change of the C atoms, slowing the reaction in the long time regime.

5. Summary and Conclusions

We investigated for the first time the phase diagram of ethylene by means of vibrational spectroscopy along the 300 K isotherm for pressures up to 5.4 GPa. The IR spectrum of the high-pressure solid-phase I is consistent with the low-temperature ambient pressure $P2_1/n$ crystal structure. The pressure-induced polymerization of ethylene occurs from this crystal phase. The kinetic analysis of the reaction and the spectra of the recovered products show that the molecular arrangement in the crystal opens different propagation paths to the polymerization of ethylene. At 3.6 GPa, the kinetic data indicate a linear growth of the polymer. This is interpreted as a polymerization occurring along a preferential direction, likely the a axis, and accordingly a crystalline high-density polyethylene is obtained. The reaction pathway closely resembles observations in the laser catalyzed polymerization at lower pressure ($P < 1$ GPa) in the liquid phase.⁶ This shows, as reported in several other cases,^{3,4,26,27} that laser irradiation and pressure increase can work as alternative tools in inducing the reaction. However, a further increase of the pressure introduces novel constraints on the sample, causing the loss of the selectivity and an increase in the dimensionality of the growth process. The spectra of the

recovered compound unambiguously show the appearance of conformational defects in the polymer. This prevents a perfect crystal packing of the polyethylene chains resulting in an increase of the amorphous fraction and thus in the formation of a lower density polymer with respect to the polyethylene obtained at lower pressure.

Acknowledgment. This work has been supported by the European Union under Contract HPRI-CT1999-00111, by the Italian Ministero dell'Università e della Ricerca Scientifica e Tecnologica (MURST), and by "Firenze Hydrolab" through a grant by Ente Cassa di Risparmio di Firenze.

References and Notes

- (1) Schettino, V.; Bini, R. *Phys. Chem. Chem. Phys.* **2003**, *5*, 1951.
- (2) Bini, R. *Acc. Chem. Res.* **2004**, *37*, 95.
- (3) Citroni, M.; Ceppatelli, M.; Bini, R.; Schettino, V. *Science* **2002**, *295*, 2058.
- (4) Citroni, M.; Ceppatelli, M.; Bini, R.; Schettino, V. *J. Chem. Phys.* **2003**, *118*, 1815.
- (5) Wieldraijer, H.; Schouten, J. A.; Trappeniers, N. J. *High Temp.-High Press.* **1983**, *15*, 87.
- (6) Chelazzi, D.; Ceppatelli, M.; Santoro, M.; Bini, R.; Schettino, V.; *Nature Mater.* **2004**, *3*, 470.
- (7) Mao, H. K.; Bell, P. M.; Shaner, J. V.; Steinberg, D. J. *J. Appl. Phys.* **1978**, *49*, 3276.
- (8) Bini, R.; Ballerini, R.; Pratesi, G.; Jodl, H. *J. Rev. Sci. Instrum.* **1997**, *68*, 3154.
- (9) Gorelli, F.; Santoro, M.; Ulivi, L.; Bini, R. *Phys. Rev. Lett.* **1999**, *83*, 4093.
- (10) Trappeniers, N. J.; Ligthart, F. A. S. *Chem. Phys. Lett.* **1973**, *19* (4), 465.
- (11) van der Putten, L.; Schouten, J. A.; Trappeniers, N. J. *High Temp.-High Press.* **1986**, *18*, 255.
- (12) van Ness, G. J. H.; Vos, A. *Acta Crystallogr.* **1979**, *B35*, 2593.
- (13) Press, W.; Eckert, J. *J. Chem. Phys.* **1976**, *65*, 4362.
- (14) Brecher, C.; Halford, R. *J. Chem. Phys.* **1961**, *35*, 1109.
- (15) Dows, D. A. *J. Chem. Phys.* **1961**, *36*, 2836.
- (16) Fan, L.; Ziegler, T. *J. Chem. Phys.* **1992**, *96*, 9005.
- (17) Takahashi, Y. *Macromolecules* **2001**, *34*, 7836.
- (18) Krimm, S. *Adv. Polym. Sci.* **1960**, *2*, 51.
- (19) Barnes, J.; Fanconi, B. *J. Phys. Chem. Ref. Data* **1978**, *7*, 1309.
- (20) Nielsen, J. R.; Woollett, A. H. *J. Chem. Phys.* **1957**, *26*, 1391.
- (21) Zerbi, G.; Del Zoppo, M. Vibrational spectra as a probe of structural order/disorder in chain molecules and polymers. In *Modern Polymer Spectroscopy*; Zerbi, G., Ed.; Wiley-VCH: Weinheim, Germany, 1999; pp 87–206.
- (22) Sano, K.; et al. *Appl. Spectrosc.* **1999**, *53*, 551.
- (23) Hulbert, S. F. *J. Br. Ceram. Soc.* **1969**, *6*, 11.
- (24) Ceppatelli, M.; Santoro, M.; Bini, R.; Schettino, V. *J. Chem. Phys.* **2000**, *113*, 5991.
- (25) Santoro, M.; Lin, J.; Mao, H. K.; Hemley, R. J. *J. Chem. Phys.* **2004**, *121*, 2780.
- (26) Ciabini, L.; Santoro, M.; Bini, R.; Schettino, V. *Phys. Rev. Lett.* **2002**, *88*, 085505.
- (27) Santoro, M.; Ceppatelli, M.; Bini, R.; Schettino, V. *J. Chem. Phys.* **2003**, *118*, 8321.